Tailoring Aspect Ratio of Gold Nano Rods: Impact of temperature, pH, silver ions, CTAB concentration and centrifugation

Goldie Oza*, Sunil Pandey*, Ritu Shah, Mayuresh Vishwanathan, Rohan Kesarkar, Maheshwar Sharon and Madhuri Sharon§

N. S. N. Research Centre for Nanotechnology and Bionanotechnology, Jambhul Phata, Ambernath (W, Maharashtra, India

---

ABSTRACT

We report synthesis strategies developed to achieve decent yield of monodispersed gold nano rods (GNR) of desired aspect ratio. The color and optical properties of gold nano particles originate from localized surface plasmons. Unlike nano-sphere the optical properties of GNR are influenced by their shape anisotropy. UV-visible absorption spectroscopic measurements and Scanning as well as Transmission electron microscopy (SEM and TEM) images provide an explanation for formation and mechanism for controlling the GNR growth. The work emphasizes on the standardization of parameters like concentration of aurochloric acid, cationic surfactant CTAB (hexadecyltrimethylammonium bromide) and silver nitrate; as well as pH and Temperature of reactant and finally efforts to separate GNR by centrifugation. Use of CTAB at 0.2M concentration and $20^0 C$ and a ratio of 200:1 of CTAB and gold salt, resulted into formation of metallo-micellar complexes. This complex acted as seed and resulted in formation of 1D crystal growth of nanorod. The most decisive parameter affecting the nucleation was found to be concentration of gold ions (1mM). Growth of GNR was mainly controlled by $AgNO_3$ (4mM) and CTAB (0.2M). Centrifugation was found to help the shape separation i.e. separating GNR from other shapes of gold nanoparticles.. A blend of theoretical as well as experimental discussion is made to comprehend the idea behind separation of the GNR from the mixture of spheres and rods.

Key words: Gold Nanorods (GNR), metallo-micellar complex, Hexadecyltrimethylammonium bromide (CTAB), aspect ratio, shape separation, centrifugation.

INTRODUCTION

The most captivating property of matter is due to the spatial movement of its electrons in the confined spaces called orbital. This electronic motion is purely dependent on the quantum mechanical principles. The dominion of confinement effect is exhibited when there is a magical transition from bulk to nanometer scale (2-10 nm); where the size of the matter becomes comparable to the Bohr exciton radius and surface effects become overriding, leading to unique absorption and fluorescent properties depending on the particle size and shape. Transition metal nanoparticles have anomalous properties, distinguishing themselves in the ability to confine resonant photons within their small size to induce localized surface plasmon oscillation of the conduction band electrons. The amplitude of the light wave gets dramatically augmented due to enhanced photonic confinement. The overall effect leads to enhancement of light intensity due to the direct relation between the intensity and square of the amplitude ($i \, \alpha \, A^2$). This effectively amplifies all radiative properties such as light absorption, florescence, Mie and Raman scattering.

Gold nanoparticles have got wider range of surface plasmon wavelengths which is a function of its size and shape [1]**.** The excitation of localized surface plasmon oscillations due to the confinement of resonant photons augments surface electromagnetic fields strongly, leading to propagation around the particles. This plasmonic near field can

stupendously affect the properties of material and molecules in its proximity leading to large enhancement of the Raman scattering by species adsorbed onto the surface of the nanoparticles. This consequently also leads to the elongation of coherent phonon oscillation of the nanoparticles and red-shift of the surface plasmon resonance band due to field coupling. The dependence of the fractional shift of the plasmon wavelength from coupled pairs of nanoparticles is purely a shape-dependent phenomenon [2-7]. The coherent oscillation in resonance with the frequency of light induces charge separation between free electrons and the ionic metal core exerting a restoring columbic force resulting in dipole oscillations. The electronic oscillations in GNR occur in one of two directions which depend on the polarisation of the incident light (short and long axes). The excitations along the short axis induce absorption in the visible region which is called as transverse band. The excitations along the long axis induce much stronger absorption band in the longer wavelength region which is considered to be known as longitudinal band. This longitudinal band is more sensitive to the aspect ratio of the GNR hence, it is shifted from visible to near infra red region (Red-shift) with increasing aspect ratio. As per Gans theory, there is a relationship between Longitudinal Surface Plasmon Resonance $\lambda_{(LSPR)}$ of anisotropic nanoparticles and aspect ratio (R) which has been mathematically found to be:

$$\lambda_{(LSPR)} = 45R + 420 \qquad\qquad (1)$$

 Due to the SPR excitations, there is five to six order of magnitude enhancement of light absorption by GNR than that of conventional dyes used for labelling and biological imaging [8-10]. The remaining light extinction is then contributed by the existence of the light scattering. This is due to the virtue of the fact that cross-section of total extinction (C_{ext}) is derived from the cross-section of absorption (C_{abs}) and scattering (C_{sca}) i.e.

$$C_{ext} = C_{abs} + C_{sca} \qquad\qquad (2)$$

The absorption scattering and total extinction of the GNR is proportional to the wavelength of light as well as particle aspect ratio. At a fixed aspect ratio, the absorption efficiency is dominant for smaller rods and scattering efficiency is dominant for larger rods. Hence, for imaging, larger nanoparticles are preferred because of higher scattering efficiency and smaller nanoparticles are used for photothermal therapy due to its higher absorption efficiency.

The next most attributing property of gold nanoparticles is the degree by which their optical properties can be tailored by altering shape, morphology and its assemblage. There is a shift of optical extinction band from the visible to near infra red region when the morphology of gold nanoparticles change from sphere to rod. Such structural and compositional tailoring can be exploited for potential *in vivo* applications where tissue absorption in near infra red window is minimal and favourable for optimal light penetration. GNRs of different aspect ratios exhibit a cardinal role in catalysis, optoelectronics, optics, photothermal therapy, reprography, single-electron transistors (SETs) and light emitters, nonlinear optical devices and photo electrochemical applications etc.

In the present work, we have prepared GNR of desired aspect ratios. These rod shaped nanostructures possess a sharp longitudinal surface plasmon peak and desirable aspect ratio which is accomplished by tuning different parameters such as pH, temperature, concentration of CTAB, gold chloride and silver nitrate solution. The effect of nitrate and silver ions were investigated to determine whether increased ionic strength plays a decisive role in rod synthesis or increased concentration of silver ions has got the monumental task of one-dimensional growth of nanorods. Further, high aspect ratio rods were separated from the mixture using centrifugation.

MATERIALS AND METHODS

Materials: Chloroauric acid (HAuCl$_4$, Molecular Weight 393.79g mol), sodium borohydrate (NaBH4), ascorbic acid, silver nitrate were obtained from Sigma Aldrich, USA. All the glasswares were washed with aqua regia and experiments were performed in nanopure water (18MΩ). GNR synthesis was done using the protocol devised by Mostafa-El Sayed [11].

Preparation of the seed: 2.5 ml of 1mM of HAuCl4 was added to 5ml of 0.2 cetyl trimethylammonium bromide (CTAB). To this solution 600µl of prechilled 10mM Sodium borohydride (NaBH4) was added under vigorous stirring condition forming pale yellow colored solution. The experiment was performed at 20^{0}C using Nanopure water (18Mohm).

Preparation of the growth solution: Growth solution of GNR was prepared by 2.5ml of 1mM HAuCl4 in 2.5ml of 0.2M CTAB. To this solution, 113µl of 4mM AgNO$_3$ and 35 µl of 78.8mM ascorbic acid were added followed by gentle agitation forming a transparent growth solution. 4µl of seed solution was transferred into unstirred growth

solution and the reaction was allowed to take place for 2 hrs. Impact of the pH was studied by varying the pH of growth solution (pH 2, 4, 6, 8, 9, 10) before addition of seed, using 1N HCl and 1N NaOH. The influence of temperature was analyzed at different temperatures (4, 20, 37, 60, 90 and 100^0C) for growth solution before the addition of seed. The comprehension of pivotal role of silver ions for one-dimensional growth of GNRs was done by varying the concentration of silver nitrate solution in the growth solution. The cardinal role of centrifugal speed for the separation of Nanorods from the mixture of rods and spheres was studied. 5ml of the solution was spun at different rotations per minute (4000, 5000, 6000, 8000 and 9000 rpm) and the samples deposited at the sides and at the bottom were analyzed to verify the extent of separation.

Characterization: The spectrophotometric analysis of the solutions was carried out using Perkin Elmer (Lambda 25) UV-Vis spectrophotometer. Morphological details of the synthesized GNR were studied using Transmission Electron Microscope (TEM) (Ziess Microimaging GmbH, Germany) and FEG-Scanning Electron Microscope (SEM) (Zeiss Microimaging GmbH, Germany). All samples were centrifuged (REMI) at 5000rpm and then both the side walls and sample present at the bottom of the centrifuge tube were separated and then placed on formvar coated copper grid for TEM analysis and on silicon wafer for SEM.

RESULTS AND DISCUSSION

The seed-mediated method for GNR synthesis was adapted from an earlier publication [12] . Synthesis of GNR was done in two steps. In step one we used sodium borohydride, which is a strong reducing and nucleating agent that reduces gold ions to form monodispersed spherical nanoparticles acting as seed for nanorod synthesis. In the second step these nuclei were then added in the solution containing CTAB (surfactant) stabilized gold complex in the presence of ascorbic acid and silver nitrate for efficient growth of one-dimensional GNR. The results obtained are discussed below:

Impact of Gold Salt Concentration in GNR synthesis:
The concentration of aurochloric acid was varied from 0.125 to 1mM. The optimum concentration of aurochloric acid required for efficient transformation of gold seeds to nanorods was found to be 1.0 mM which is evident from UV-Vis spectra exhibiting Transverse and Longitudinal Surface plasmon resonance at 525nm and 672nm respectively. According to equation (1) the aspect ratio was calculated to be 5.6 which was further confirmed by SEM. The interaction of Au (III) and CTAB efficiently leads to the synthesis of Au (III)-CTAB metallomicellar complex. It was deciphered that the ratio of CTAB: Au (III) should be 200:1 for nanorod synthesis ratio higher than that leads to unregulated growth of nanoparticles leading to irregularly shaped nanostructures (Fig. 1 and 2A). When CTAB concentration was far above critical micelle concentration i.e. 1 mM and the ratio of CTAB: Au (III) was more than 10:1, it lead to solubilization of gold ions into CTAB forming a strong micellar complex. As this ratio is further increased to 200:1, there was proficient growth of nanorods allowing addition of gold ions at specific facet regulated by the zipping mechanism of CTAB.
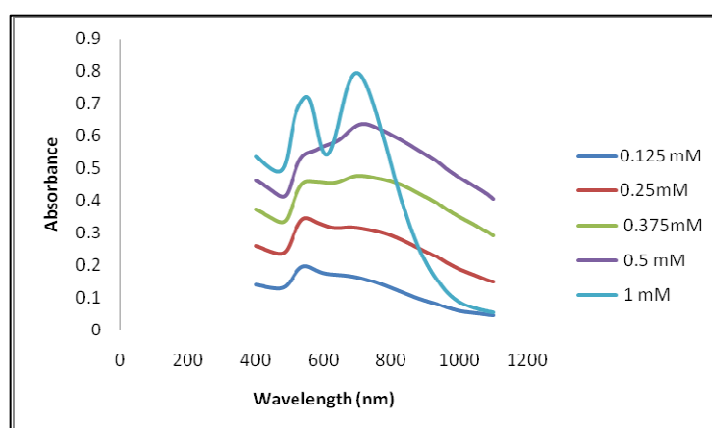

Figure. - 1. UV- Vis spectra of GNR synthesized by varying the concentrations of the gold salt in growth solution
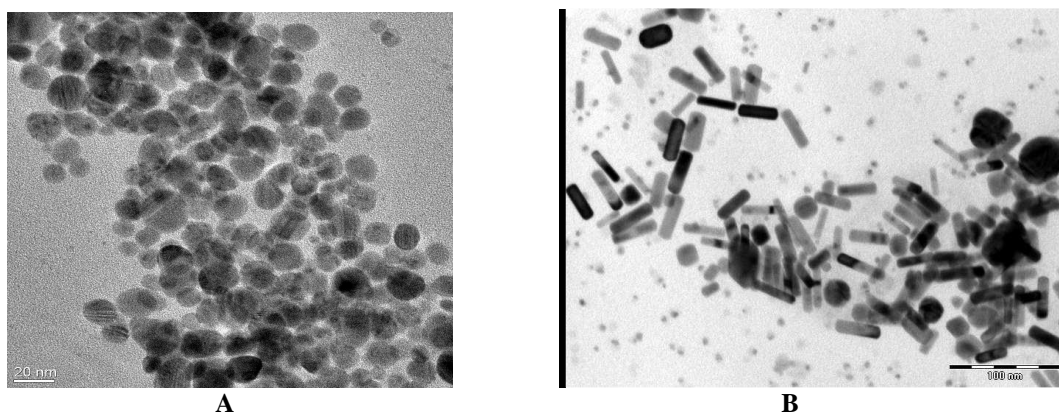
<div align="center">A   B</div>

Figure. - 2. TEM of GNR synthesized using (A) 0.125 mM and (B) 1.0 mM Aurochloric Acid

Effect of Cetyl Trimethyl Ammonium Bromide (CTAB)

Our initial experimental studies as well as reports [13] have depicted that 20^0 C is the most suitable temperature for studying the impact of various reactants during synthesis of GNR. Hence, impact of CTAB was assessed at 20º C. For our experimental considerations, GNRs were synthesized using different concentrations (0.004, 0.008, 0.1, 0.2, 0.3, 0.4 and 0.5 M) of cationic surfactant CTAB. In accordance with the previous endeavours to unlock the interaction of CTAB with the surface of GNR, optimum results were obtained 0.2 M CTAB at 20°C. To decipher the optimum CTAB concentration in the growth solution keeping all the other experimental parameters constant, different CTAB were varied from 0.004 M to 0.5 M. The UV-Vis spectrophotometric analysis of the gold nanoparticles as well as TEM (Fig. 4), evidently indicates that 0.2 M CTAB is most effective in synthesising GNR, having an aspect ratio of 3.5 (Fig. 4b). We speculate that at this CTAB concentration there is inhibition of extra growth at 111 facets of GNR. This leads to the proper elongation of 1D growth of nanorods. This is in agreement with earlier work [13] that has unravelled the mechanism of CTA^+ bilayer protection [14]. As CTAB concentration is lowered down from 0.1 M to 0.008 M, there has been catastrophic decline in LSPR as well as alteration in morphology of gold nanoparticles (Fig 4 C & D).

Earlier experiments [15] have determined the critical micelle concentration of (CMC) CTAB to be □ 1mM. We have investigated the effect of CMC on nanorod growth at 20 °C by using CTAB concentration from 0.1 to 1 mM and have gained an insight into the role of metallo-micellear complexes behind the formation of 1D crystal growth of nanorod. Above CMC, it has been noticed that $(AuCl_4)^-$, which was a pale yellow colored solution, formed orange colored precipitate, when complexed with CTAB. Appearance of this color is a clear indication of water insoluble Au-surfactant complex solubilised into micelle. As the concentration of CTAB increases from 0.004 M to 0.5 M, the formation of orange colored precipitate disappears. The amalgamation of CTAB and $HAuCl_4$ in aqueous solution results in the formation of CTA - $[AuBr_4]^-$, an organic salt which is solubilized by the surfactant micelles to form metallo-micelles [16].

The role of CTAB in the formation of GNR can be speculated as follows:

a) It has got very high affinity towards gold salt, thus forming a very strong complex leading to the retardation of reduction process.

b) It protects instant reduction of Au^{+3} by caging the complex inside the micelle (Fig. 3).

c) The vectorial growth of nanorod is possible due to the preferential adsorption of CTAB on its surface [17].
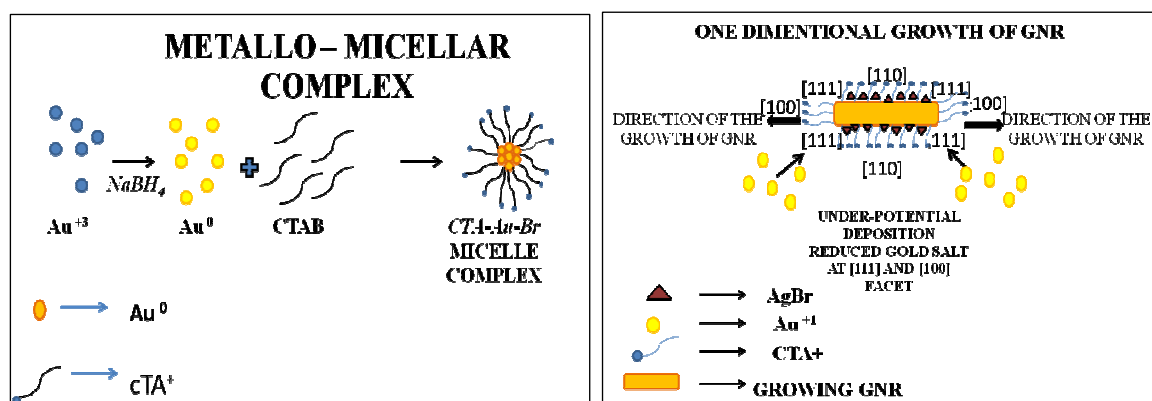

Fig. 3 – Schematic diagram exhibiting the Zipping mechanism of gold and CTAB micelle

The increasing CTAB availability leads to the formation of double layered structures called micelles, within which the crystal growth occurs [18] . The above reaction happens at 20°C at which CTAB is expected to exist as single layer micelle with the ammonium group in contact with the surrounding water molecules and the hydrophobic tail directed inwards in to the micelle. Since the "Kraft point" of CTAB is around 20°C, the synthesis of GNR with high aspect ratio is possible [19].

$$[AuCl_4]^- + 4CTAB \leftrightarrow CTA\text{-}[AuBr_4]^- + 4Cl^- + 3CTA^+$$
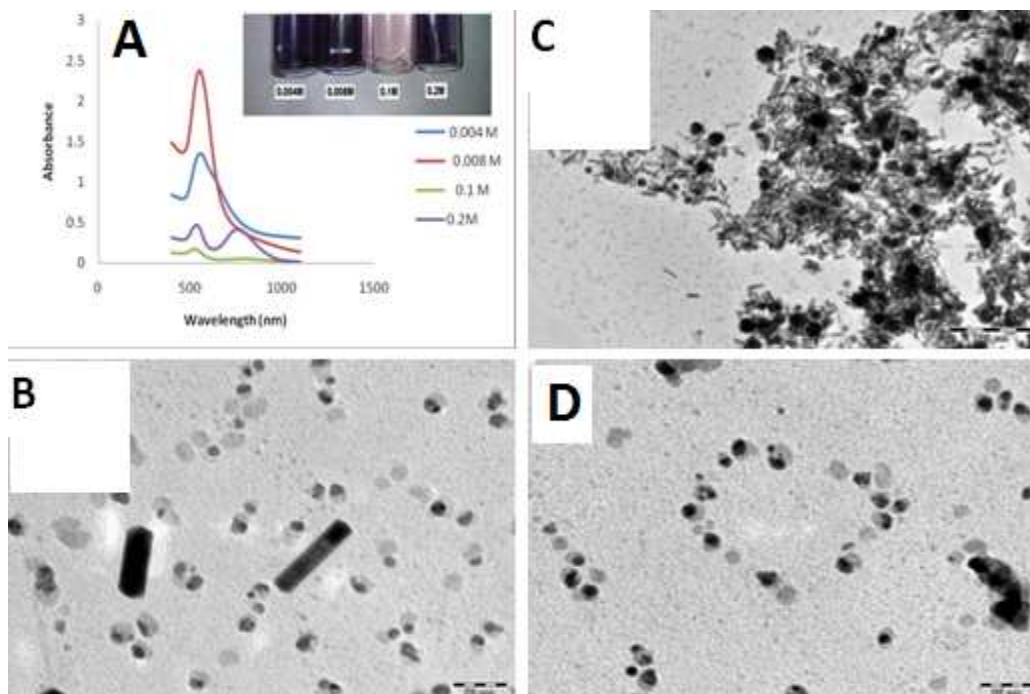
Figure. 4 – Gold nanoparticle formation using different concentrations of CTAB(A) UV-Vis spectra and TEM image of GNR synthesized using (B) 0.2 M (C) 0.1 M and (D) 0.008 M CTAB.

The shape anisotropy exhibited by GNR in the presence of CTAB is determined by symmetry reduction which is correlated to cyclic penta-twining of the FCC lattice. The transformation from spherical isotropic seeds to anisotropic growth of the isometric penta- twined nanoparticles leads to the rapid elongation along the common 110 axis, evidently the process is autocatalytic [13, 20,] .
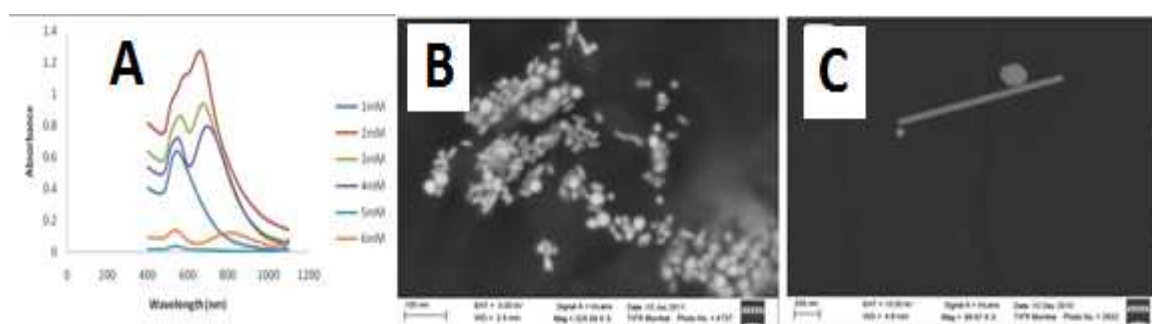

Fig. 5 - Gold nanoparticle formation using different concentrations of Silver Nitrate (A) UV-Vis spectra; and SEM image of GNR synthesized using (B) 4 mM and (C) 6 mM AgNO₃

Impact of Silver Nitrate on GNR Synthesis:
The impact of silver nitrate was studied using different concentrations 1, 2, 3, 4, 5 and 6 mM in growth solution can be deduced the UV-Vis-spectra (Fig. 5A) that spherical nanoparticles were synthesized when 1 and 2 mM silver nitrate was added whereas addition of 4mM silver nitrate caused GNR synthesis of high aspect ratio. Further, increment in the silver concentration (5 and 6 mM) lead to red shift of LSPR causing increased aspect ratio (Fig. 5c). The optimum silver concentration for GNR synthesis was found to be 4mM since at this concentration; growth occurs from a specific facet and allows directed growth of rods. In the presence of CTAB, the empty facets of GNR-

CTAB interface allow unregulated deposition of gold in the growth solution leading to the formation of penta-tetrahedral twined structures having aspect ratio in the range of 3-4.

To confirm whether the tuning GNR of desired aspect ratio is due to silver or nitrate; a trial using potassium nitrate salt (4mM) was performed. It was found that as the ionic strength increases, there is drastic transformation from anisotropic structure to spherical nanoparticles. The UV-Vis spectra depict the pivotal role of silver ions in the growth of GNR. However, the impact of potassium nitrate was inhibitory to GNR synthesis. In presence of potassium nitrate, the absence of LSPR confirms that the nanorod formation is prevented. Moreover, it is only silver ions which play critical role in nanorod synthesis and not the nitrates. The results obtained by spectral analysis were consistent with electron micrographs shown (Fig. 6).
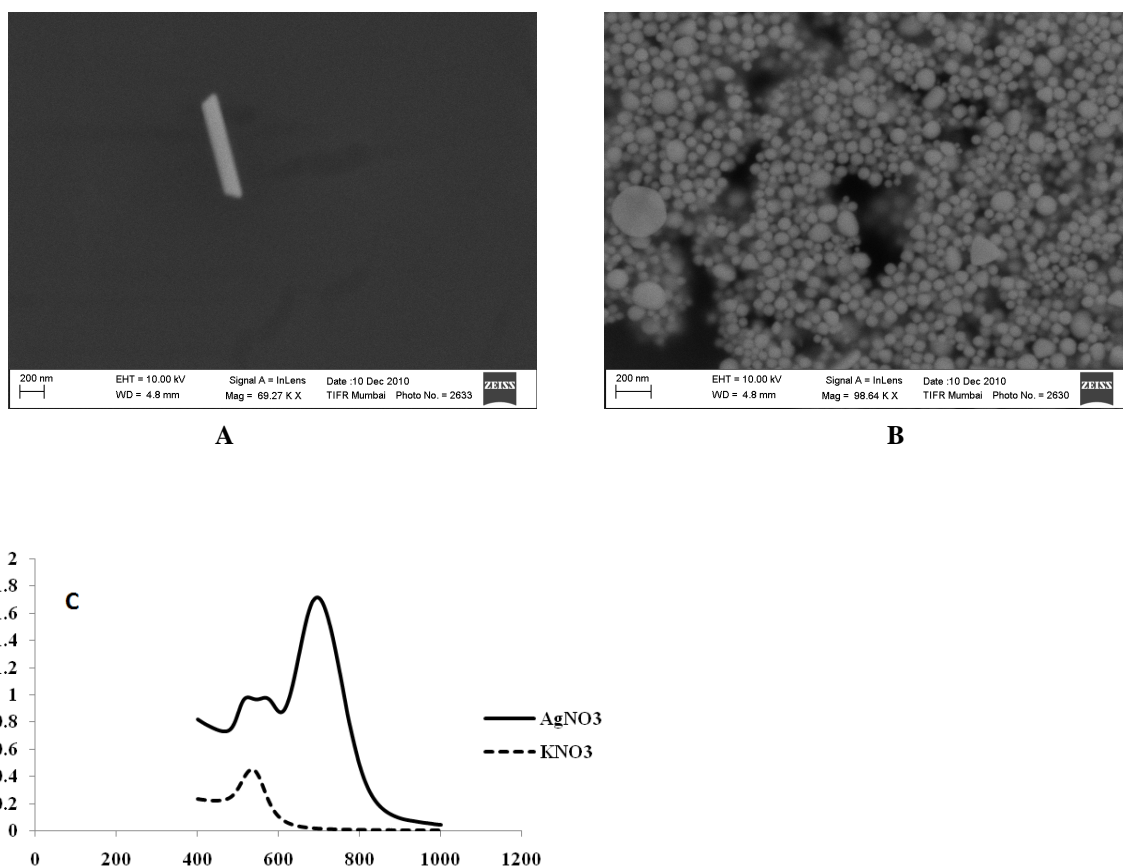
Figure. 6 – SEM of GNR formation (A) in the presence and (B) in absence of Silver Nitrate and (C) supporting evidence for both by UV-Vis spectra

At low pH, ascorbic acid weakly reduces silver ions. However, complete reduction to Ag (0) is not possible. Hence, it is proposed that there is formation of AgBr during GNR growth [21]. AgBr plays dominant role in the synthesis of stabilized GNR by getting deposited on 110 facets of rod surfaces at the gold-CTAB interface (the concentration of AgBr is higher than K_{sp} of the bulk silver bromide) [22] . This facilitates directed growth of GNR from a specific facet which is less densely covered by CTAB or AgBr, thus hindering unregulated deposition of Au atoms on the whole seed surface. Silver (Ag0) is also formed in small concentrations which creates a monolayer on the gold-CTAB interface due to interfacial deposition [23,24].
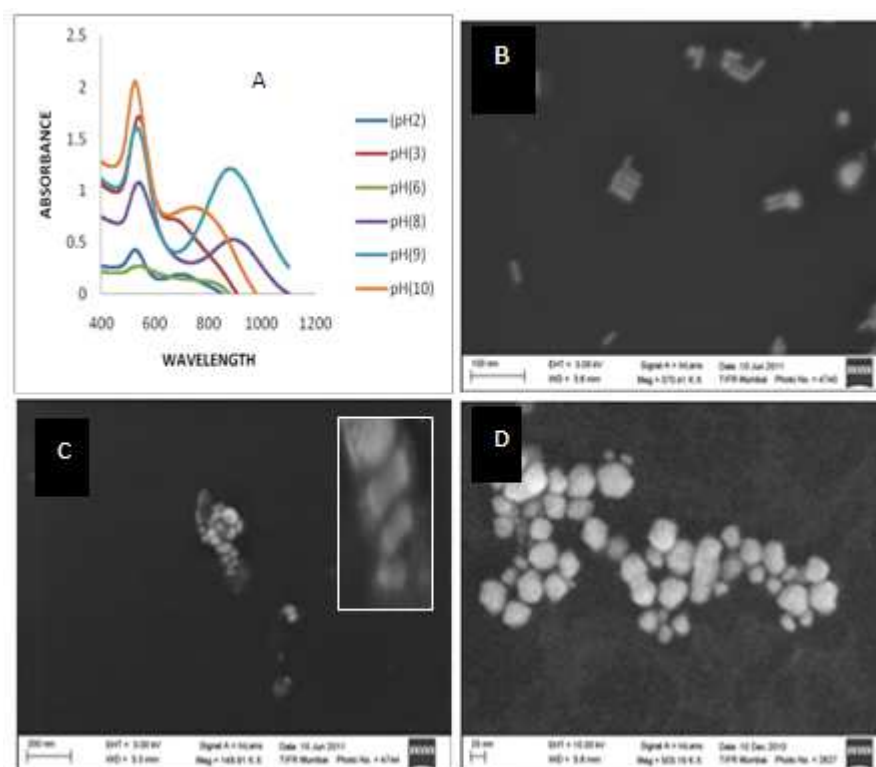
Impact of pH on GNR Formation:
UV-Vis spectra of GNR with growth solutions of different pH (2.5, 3, 4, 6, and 9) were recorded (Fig. 7). At lower pH (2.5 & 3), the samples exhibited both TSR and a tuneable LSR peak. As the pH of the solution was increased, the spectra showed only one peak between 500 – 600 nm indicating the formation of spherical nanoparticles. The Gaussian shape of LSPR was lost when pH was more than 5. The shape and size of the nanoparticles were further confirmed using TEM showing rods of high aspect ratio at pH 2.5 with flat tips. We contemplate that the increment in the pH leads to the disappearance of the rod shaped gold nanoparticles and also increase in the sphericity of the nanoparticles. It was observed that the optimum pH for GNR synthesis was 2.5 which was the inherent state of the

growth solution for stable GNR synthesis. However, at pH 3, there was blue shift in the LSPR peak which significantly implies that morphology of the GNR becomes bone like (inset in Fig. 5C) and hence the aspect ratio decreases.

The real jugglery behind the cardinal role of pH in fabrication of longer GNRs is slow reducing capacity of the weak reducing agent ascorbic acid used in the growth solution in seed mediated synthesis of GNR. At lower pH, the weak reducing potential of ascorbic acid results in slow reduction of Au (III) to Au (I). When seed solution is added into such solution, further reduction of Au (I) to Au (0) occurs, allowing its preferential deposition on to the facets of seed nanoparticles. The weak reduction potential of ascorbic acid (+ 0.252V) at pH 2.5 may not completely reduce silver ions to Ag (0) leading to the proposal of a different mechanism for GNR synthesis as discussed earlier in 2.3. Additionally, at low pH, the increased repulsion between GNR due to high concentration of H^+ in the solution facilitates the growth of GNR of higher aspect ratio [21].

The reducing capacity of ascorbic acid is not the most attributable feature affecting GNR synthesis at different pH, but CTAB also plays a magnificent role in the formation of GNR with variation in pH values. Based on the report by Pal and co-workers [23] it was speculated that as pH rises, the diameter of CTAB micelle decreases thus, creating a barrier for one-dimensional crystal growth. CTAB concentration of 0.2M is much higher than the CMC at which regulated and one-dimensional faceted growth of tips occurs. At the optimum concentration (0.2M) and inherent pH (3.5), CTAB acts as a soft scaffold and the diameter of the micelle becomes meticulous enough to allow GNR synthesis.

Figure. 7 – Impact of pH on formation of GNR as studied using (A) UV-Vis spectrophotometry showing GNR peaks at pH 2 and SEM of GNR synthesized at (B) pH 2 (C) pH 3, also showing bone shaped gold nanoparticles in inset and (D) 10

As a matter of fact, the comprehension of the modus operandi of alteration in the size and morphology of GNRs with variation in pH needs a critical scrutiny with the assistance of a mass flow of information from the literature. It has been proposed from the earlier works that GNRs prepared by silver ion-assisted seed mediated method possess four side surface with {110} facets and mainly {100} and {111} facets at its tips [22, 23, 24]. Since the surface energy of 110 facet is higher than {100} and {111} facet, this results in the adsorption of CTAB bilayer onto the 110 facet [24, 25, 26]. This prevents the interaction of gold atoms on such CTAB stabilized facet thus allowing its preferential deposition onto 100 and 111 facets forming rod-shaped nanoparticles ((Fig. 8). Furthermore, when silver nitrate is added into the growth solution, due to low pH as already mentioned above, silver bromide (AgBr) would selectively adsorb onto the 110 facet of gold nanoseeds. This navigates the deposition of gold atoms onto the 100

facets of the gold nanoseeds. Thus, dense packing of CTAB bilayers and AgBr on 110 facets pilots the deposition of gold atoms on (100) [23] facet thus forming longer and longer rods. But with increase in the pH, there is catastrophic deterioration in CTAB capping on (110) facet, resulting in the vulnerable deposition of gold atoms on such facets forming thermodynamically favorable spherical or ellipsoidal nanoparticles. As suggested [23. 27, 28] he alkalinity of the solution results in the replacement of bromide ions with hydroxyl ions or ascorbate ions to adsorb on the micelle surface and form smaller CTAB micelles. This desorbs CTAB molecules from the gold surface allowing growth on the sides of gold nanoparticles forming spherical nanostructures.
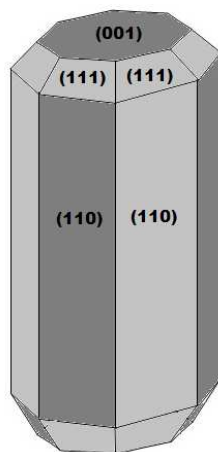
Fig. 8 – Schematic representation of GNR showing its different facets

Impact of Temperature on Fabrication of GNR
The comparative spectra and transmission electron micrographs at different temperatures (Fig 8 A & B and Fig 9 A-D) signify the decrease in the longitudinal plasmon resonance peak with increase in temperature. At 37°C, the $_{LSPR}$ at 743 nm shows the highest aspect ratio of 3.41, which is uppermost among nanorods synthesized at all other temperatures. At lower temperatures (4 and 22^0 C) there is homogeneity, in the morphology of gold nanoparticles. As the temperature increases, there is drastic change in the morphology of the particles exhibiting the dominance of cubical and triangular nanostructures which can be confirmed by the appearance of longitudinal peaks during the spectroscopic examination (Fig.9A). An exorbitant feature of the plot derived from the aspect ratio Vs temperature (Fig. 9B) is the declining aspect ratio with respect to temperature. Also, the nanorods at this temperature exhibit considerable monodispersity as seen in the TEM image (Fig. 10). With increase in temperature, the aspect ratio reduced to minimum at 100°C (aspect ratio 2.1). As shown in the TEM image, at 100°C the concentration of nanospheres is dominant over rods (< 30 % GNR).


A	B
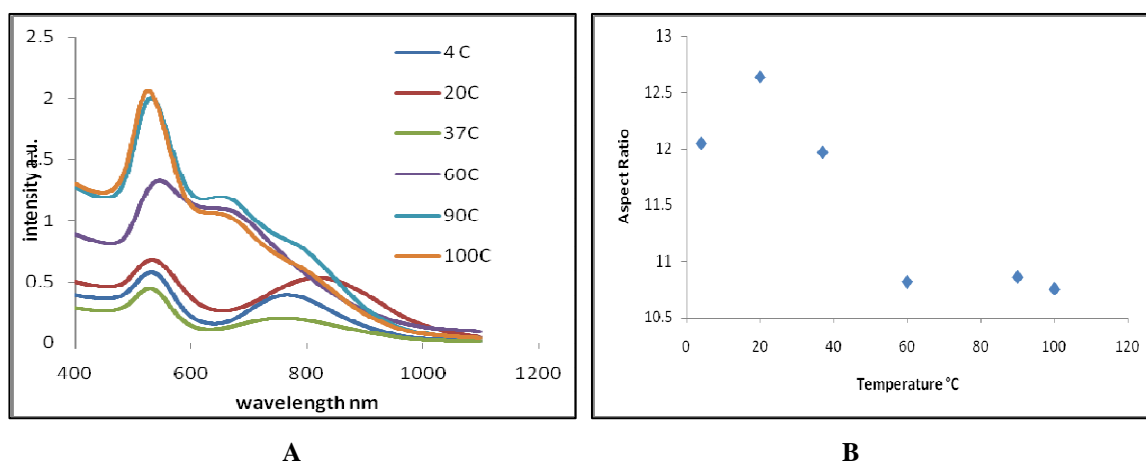
Fig. 9 - (A) Comparative UV spectrophotometric analysis of GNR at different temperatures (4°C, 20°C, 37°C, 60°C, 90°C and 100°C), (B) Plot of Temperature versus Aspect Ratio showing maximum aspect ratio of 12.64 at 20 °C after which there is decrement in the aspect ratio as the temperature increases from 60°C to 100°C

However, the exact quantification of the GNR yield was not done. The nature of the graph in fig. 9A shows consistent blue shift from 743nm to 622nm. The distinctive morphology and optical behavior of the GNR at gradients of temperature ranging from 4°C to 100° C can be explained considering two most fundamental attributes

restricted to the colloidal interactions at different temperatures. These two fundamental features are the enhanced molecular agitation and thermal fluctuations leading to the massive molecular disorderness (increased entropy) [16, 17]. The second aspect is critical micelle concentrations of cationic surfactant CTAB at different temperatures. CTAB has a "Kraft point" at 20°C which is the temperature at which micelles are formed. The double layered structure created by CTAB, allows uniquely shaped crystal growth to occur. The stability of GNR is dependent on the physicochemical parameters such as CTAB concentration at20°C. At 4^0C, the CTAB exist as single layer micelles with ammonium groups interacting with the surrounding water molecules and the hydrophobic chains bound to GNR. With increasing temperature the impact of entropy, as mentioned earlier, becomes dominant leading to the destabilization of the micellar structure. This augments the concentration of CTAB to form more and more double layered structures which is significant for the synthesis of GNR. This is due to the fact that more surfactant molecules become available at temperatures above 37^0C, thus supporting crystal growth along the 1D axis resulting in higher aspect ratio. Furthermore, increment in the temperatures above 80^0C leads to increase in thermal disorderness, thus reducing the aspect ratio of the GNR [17]
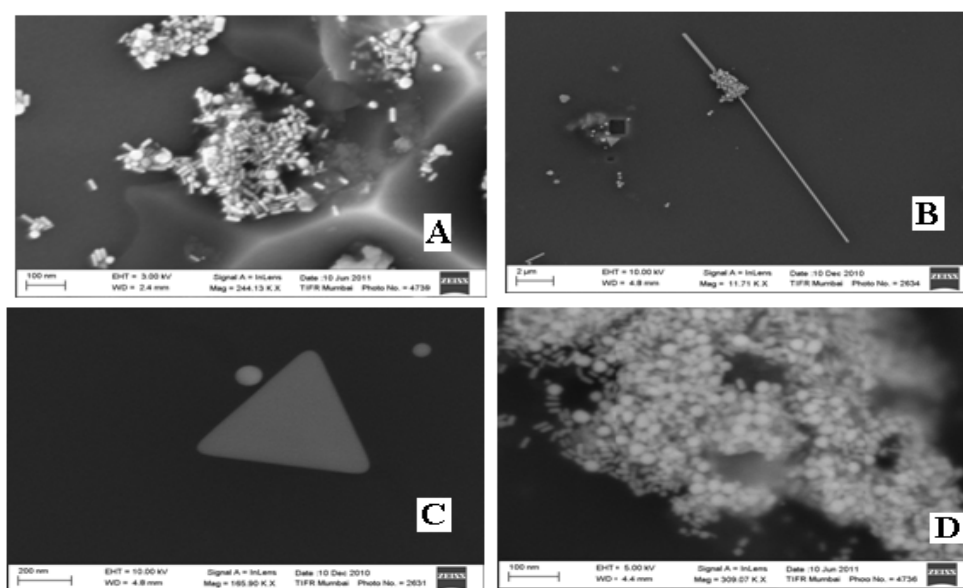
Fig. 10 - Transmission electron microscopic image of gold nanoparticles exhibiting the influence of (A) 20 °C , (B) 37° C , (C) 80° C and (D) 100°C

*Impact of Centrifugation at Different Rotations per Minutes on GNR*

There is considerable heterogeneity in the shapes of gold nanoparticles in the solution made with an intention to fabricate nanorods specially using seed mediated method (Fig. 12a &b) These mixtures of GNR as well as spheres make considerable impact on the sedimentation rates of gold nanoparticles, making it a complex multy body interaction problem . Under such critical circumstances, the separation of GNR from mixture of spheres and rods becomes a daunting task. Predictions of a concrete equation, particularly in the quest of separating nanorods, require non equilibrium thermodynamics which remains a difficult task even for spherical nanoparticles [29]. This is mainly due to: (a) Ever-changing reactions and shape transitions in the solution of gold nanoparticles (b) Heterogeneous nature of the solution (c)The knowledge of exact kinetics of the rates of reactions and (d) Entropic constraints due to increased Brownian motion.

However, the results were not consistent at all the rpm. This may be due to difference in surplus of parameters which play fundamental role during centrifugation of dilute colloidal solutions.

The mother gold colloidal solution was synthesized by modifying Mostafa El Sayed's protocol. In order to examine the impact of centrifugation a set of 5 ml of GNR solution was subjected to the centrifugation speed from 5,000 to 9000 rpm. The comparative study of the morphology as well as spectroscopic properties was gauged by using Transmission electron Microscopy (TEM) (Techne) and UV-Vis spectroscopy (Perkin Elmer Lambda 25).

The mother solution before centrifugation, as seen after the spectroscopic studies, exhibited two sharp peaks at 530 and 779 nm corresponding to the TSR and LSPR of the GNR respectively. The striking feature of the spectra is feeble absorption intensity at both the peaks. This mixture shows the presence of spheres as well rods as seen in the TEM image (Fig. 12 a & b). After the centrifugation at 5000 rpm, there is slight separation of the GNR at the side

wall. The spectrum shows higher intensity of TSR with a slight red shift from 779 to 830 indicating the presence of high aspect ratio GNRs. However, there is more concentration of the gold nanospheres than nanorods as confirmed by the TEM which is improved situation than mother solution (Fig. 12 c & d). The impact of 8000 rpm was noteworthy. The spectrum explains the presence of strong LSPR with red shift. The TEM image shows the high percentage of the GNR with moderately high aspect ratio. As the centrifugation speed increases the spectrum gets distorted due to the destabilization of the GNR as CTAB double layer gets disrupted resulting in the removal of high concentration of CTAB in the solution. Even, the spectroscopic scrutiny of the pellet settled at bottom shows the presence of dual peaks and both gold nanospheres and nanorods in the TEM image. The presence of the rods at the bottom is due to the fact that shorter and thicker rod settles down at the bottom rather than at the side walls as per the theoretical explanations[30] .As per our earlier theoretical confrontations, the behavior of nanoparticle in a solution is purely a function of effective mass and friction coefficients. In a comparative mathematical calculation considering the ratio of effective mass and friction coefficients, the ratio of velocities of rods and spheres under the influence of centrifugal field, is chiefly regulated by the relative diameters of the particles. This justifies the presence of rods on the sides of the tube.
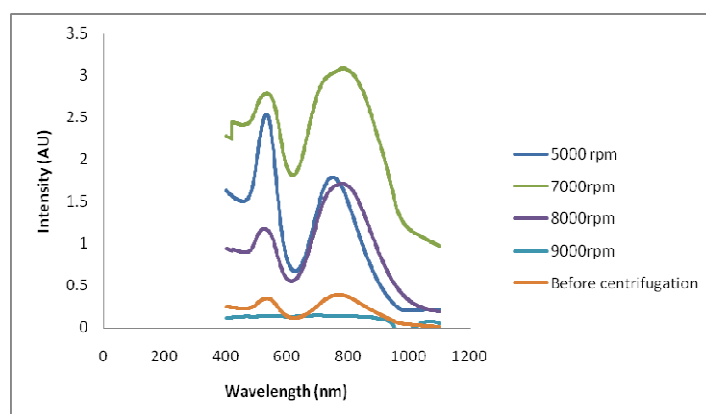
Figure. 11 - Surface plasmon resonances of GNR at different centrifugal speeds and graph showing aspect ratio at different values of LSPR
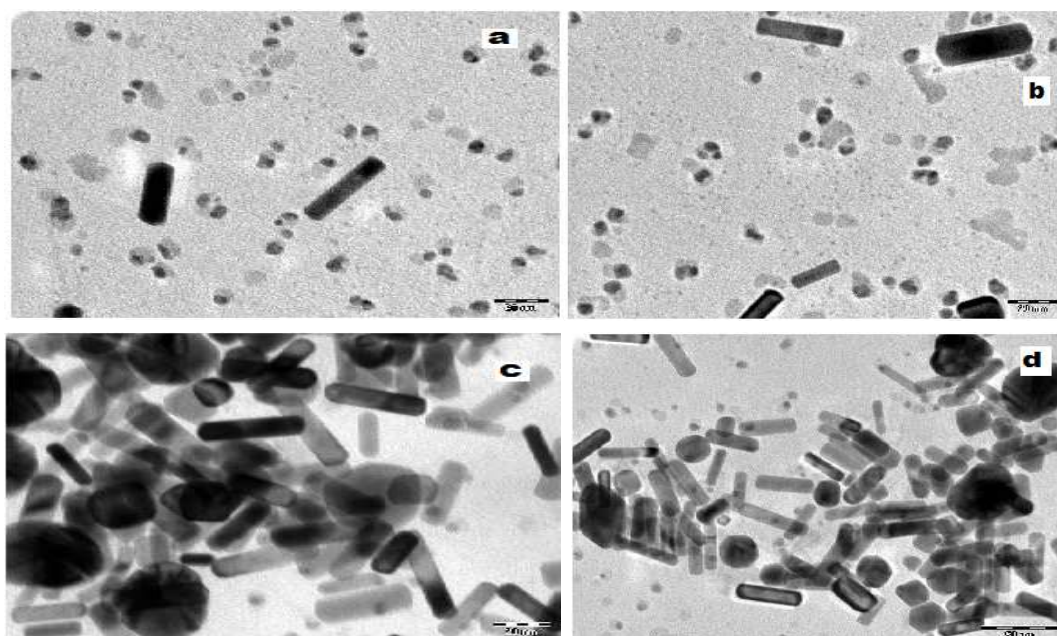
Fig. 12 - Transmission electron micrograph of GNR (a &b) before centrifugation and samples centrifuged at (c) 5000rpm and (d) 8000 rpm

In order to unravel the theory behind such results, we need to consider the fundamental difference when a rod and a sphere are subjected to centrifugal force. The difference in the shapes imposes a very important parameter which needs to be considered called friction factor. At nanoscale, the friction can be explained by Reynolds number (*Re*).

1036

For sedimentation problems arising at nanoscale Re $\Box$1(life at low Reynolds number). Reynolds number ($Re = \rho UL/\eta$) is dependent on viscosity (η), density of the fluid (ρ) and most importantly speed of centrifugation in our case (U) and length of the nanoparticles (L). In short, this property is interplay between inertial and viscous forces. The coefficient of frictions, which is a function of Reynolds number, is same for spherically isotropic nanoparticles (Ramaswamy, 2001). In a broader sense, spherically isotropic nanoparticles consist of all polyhedral, cubic, icosahedral and octahedral structures leaving behind nanorods for a separate treatment in order to comprehend its sedimentation properties. In case of nanorods the friction coefficient is dependent on the alignment of the nanorods during the synthetic procedure. This is by the virtue of the fact that the friction experienced parallel to the rod is half of the transverse collapsing rods [31, 32. 33.34,35]. In a stark contrast to the settling property of the spherical nanoparticles which settle in the direction of the gravity anisotropic nanoparticles, because of the impact of Brownian storm, sediment at an angle to the direction of the effective gravity which can deviate up to 19.5° in case of a thin nanorod [35]. Moreover, orientation of GNR in the solution plays pivotal role under the influence of gravity as well as centrifugal force. In the solution the continuous dynamic status of nanorods having equal dimension due to the influence of intense Brownian fluctuations forces them to sediment at a distance comparable to their length. This theory also supports the unequal spatial distribution of spheres as well as rods after centrifugation.

In a solution containing heterogeneous mixture of anisotropic particles, the dynamics of surrounding particle accelerates the velocity of the particle. This mosaic of particle interactions (Hydrodynamic interactions) makes the sedimentation velocity as an additive property of sedimentation velocities of single spheres. Moreover, the thermal diffusion or Brownian movement influences the sedimentation of a particle during centrifugation. Further, Self-Sharpening effect enhances the sedimentation speed of the particles which lag behind due to the concentration dependence of the drag thus separating different and unique sized particles [30].

CONCLUSION

It can be concluded that Gold Au (III) forms metallo-micellar complex with CTAB resulting into stable gold nuclei, which is used as a scaffold for Nanorod synthesis. In the growth solution, after addition of optimum concentration of Au (III) – CTAB, reduction of Au (III) to Au (I) is possible due to Ascorbic acid. Further gold seeds reduce Au (I) to Au (0). Due to low pH, low reduction potential of Ascorbic acid further reduces Silver ions to Silver bromide which can occupy (110) facet of gold nanorod allowing only one-dimensional growth at the tips. The role of nitrate was completely ruled out for GNR formation as it formed Spherical nanoparticles only in the absence of Silver and presence of Potassium nitrate. The temperature of the whole reaction system was kept at 20ºC which is the "Kraft point" of CTAB allowing suitable solubilization of gold ions into the surfactant forming micelle. Finally, a pertinent method to separate GNRs from other shapes using centrifugation is developed. It is due to the influence of centrifugal force that rods were deposited at the sides of the centrifuge tubes and larger rods along with nanoparticles of other shapes were found at the bottom of the tube.

REFERENCES

[1] AJ Haes, DA Stuart, S Nie, RP Van Duyne, *J. Fluoresc* , **2004**,14, 355
[2] PK Jain, W Huang, MA El-Sayed, *Nano Lett*., **2008,** 8, 4347
[3] PK Jain, MA El-Sayed MA, *J. Phys. Chem C*, **2008** 112: 4954–4960
[4] PK Jain, MA El-Sayed, *Nano Lett.,* **2007,** 7:2854
[5] X. Huang, P.K. Jain, I.H. El-Sayed, M.A. El-Sayed.. *Nanomed.* **2007**, 2(5), 681
[6] PK Jain, W Huang, IH El-Sayed, MA El-Sayed, *Acc. Chem. Res.,* **2008,** 41:1578
[7] C Tabor, R Murali, MA Mahmoud, MA El-Sayed. *J. Phys. Chem. A*, 2**009,** 113,1946
[8] PK Jain, KS Lee, IH El-Sayed, MA El-Sayed *J. Phys. Chem. B*, **2006** 110:7238
[9] LD Landau, EM Lifshitz, Electrodynamics of Continuous Media, 2nd edition, Elsevier Science & Technology, Oxford, UK, **1984**
[10] HC Van de Hulst, Light Scattering by Small Particles, Wiley, NewYork, **1957**
[11] B Nikoobakht, MA El-Sayed MA (**2003**) Preparation and Growth Mechanism of Gold Nanorods (NRs) Using Seed-Mediated Growth Method. *Chem. Mat.* 15:1957
[12] NR Jana, L Gearheart, CJ Murphy, *Journal of Physical Chemistry B*, **2001,** 105,4065
[13] Y Tang, B Du, J Yang, Y Zhang, *J. Chem. Sci*., **2006,** 118, 281

[14] K Torigoe, K Esumi, *Langmuir,* **1992,** 8,59

[15] V Sharma, K Park, M Srinivasarao, *Materials Science and Engineering R,* **2009,** 65,1

[16] J Pérez-Juste, I Pastoriza-Santos, LM Liz-Marzán, P Mulvaney, *Coord. Chem.Rev.,* **2005,** 249,1870

[17] R Becker, B Liedberg, PO Käll, *Journal of Colloid and Interface Science,* **2010,** 343,25

[18] CJ Murphy, TK Sau, AM Gole, CJ Orendorff, JX Gao, L Gou L, SE Hunyadi, T Li, *J. Phys. Chem. B*, **2005,** 109, 13857

[19] M Grzelczak, J Perez-Juste, P Mulvaney, LM Liz-Marzan, *Chem. Soc. Rev.* **2008,** 37, 1783

[20] F Hubert, F Testard, O Spalla, *Langmuir,* **2008** , 24, 9219

[21] MZ Liu, P Guyot-Sionnest, *J. Phys. Chem. B*, **2005,** 109, 22192

[22] CJ Orendorff, CJ Murphy, *J. Phys. Chem.B*, **2006,** 110,3990

[23] T Pal, NR De Jana, N Pradhan, R Mandal, A Pal, AE Beezer, JC Mitchell, *Langmuir* , **1998,** 14, 4724

[24] HA Keul, M Möller, MB Bockstaller, *Langmuir,* **2007,** 23, 10307

[25] TS Sreeprasad, AK Samal, T Pradeep, *Langmuir,* **2007,** 23, 9463

[26] ZL Wang, RP Gao, B Nikoobakht., MA El-Sayed, *J. Phys. Chem. B,* **2000,** 104, 5417

[27] W Chungang, T Wang, MA Zhanfang, SU Zhongmin, *Nanotechnology*, **2005,** 16, 2555.

[28] H Topallar, B Karadag, *J. Surfactants Deterg*, **1998,** 1, 49

[29] H Fujita, Foundations of Ultracentrifugation Analysis (Wiley, New York), **1975**

[30] S Ramaswamy, *Adv. Phys.,* **2001,** 50(3), 297

[31] V Yogesh, VS Marathe and V S Shrivastava, *Advances in Applied Science Research*, **2011**, 2 (3),295

[32] J Happel, H Brenner, Low Reynold Number Hydrodynamics (Noordhoff International Publishing, Leyden, The Netherlands), 2nd Ed, pp 219–220. **1973**

[33] Z Dogic, AP Philipse, S Fraden, JKG Dhont, *J. Chem. Phys,* **2000,** 113, 8368

[34] TGM Van de Van, Colloidal Hydrodynamics (Academic, London), pp 268–272. **1989**

[35] JM Peterson . *J. Chem Phys,* **1964,** 40,2680